HERMETIC PACKAGES AND FEEDTHROUGHS FOR NEURAL PROSTHESES

Quarterly Progress Report # 10
(Contract NIH-NINDS-N01-NS-4-2319)
(Contractor: The Regents of the University of Michigan)

For the Period:
January-March 1997

Submitted to the

Neural Prosthesis Program
National Institute of Neurological Disorders and Stroke
National Institutes of Health

By the

Center For Integrated Sensors and Circuits
Department of Electrical Engineering and Computer Science
University of Michigan
Ann Arbor, Michigan 48109-2122

Program Personnel:

UNIVERSITY OF MICHIGAN
Professor Khalil Najafi: Principal Investigator

Graduate Student Research Assistants:
Mr. Anthony Coghlan: RF Telemetry & Microstimulator Assembly
Mr. Mehmet Dokmeci: Packaging and Accelerated Testing
Mr. Jeffrey Von Arx: Electrode and Package Fabrication/Testing

VANDERBILT UNIVERSITY
Professor David   L. Zealear, Principal Investigator

April 1997

SUMMARY

During the past quarter we continued testing of glass packages under accelerated conditions, continued the characterization of the receiver circuitry for the single-channel microstimulator and assembled a few microstimulators using the old circuit chips, and completed the design and simulation of a fully integrated multichannel nerve stimulation system.

Our most significant package testing results to date are those obtained from a series of silicon-glass packages that have been soaking in DI water at 85°C and 95°C for more than a year. We reported in the last progress reports that all packages soaking at 95°C had failed. There were also 4 packages that were soaking at 85°C. All these four packages are still dry and under test. Of the original 10 packages, the longest going sample has reached a maximum of 961 days at 85°C and 484 days at 95°C. If we assume that all of the packages at 85°C failed the same time that the 95°C packages failed (obviously this is not the case, but for purposes of obtaining a more realistic mean time to failure for these packages we make this assumption), we can calculate a worst case mean time to failure of 258 days for the samples at 85°C, and of 119 days for the samples soaking at 95°C. The worst case MTTF at body temperature based on these tests is then calculated to be 59 years. These tests have been very encouraging and clearly indicate the packages can last for many years in water. In addition to these tests in DI water, we had also soaked several packages in *saline* at the above two temperatures. The results obtained from these tests were reported in the last progress report. We will continue to perform high-temperature tests in saline in the coming quarter once we have determined an effective way of preventing silicon dissolution at these higher temperatures. We also have had 4 packages soaking at room temperature in saline. The longest lasting package has been soaking for 863 days, and an average soak period of 716 days at room temperature. We will continue to observe these packages for any sign of leakage.

We also tested the glass-silicon packages to measure bond strength. These pull tests indicate that the glass-silicon bond is stronger than either the glass or the silicon and that the overall mechanical strength of the package is about 5MPa on average. This is consistent with other results reported in the literature.

During the past quarter we continued the characterization and testing of the receiver circuitry for the microstimulator. We have been trying to determine the source of excessive leakage in this circuitry, and have still not been able to conclusively determine the cause. Testing is continuing at this point in time. We have made some changes to the layout to make the circuit even more robust. A new set of wafers will be fabricated in the summer. A few single-channel microstimulators were assembled using the old circuit chip and larger receiver coils, and were encapsulated using silicone rubber. They demonstrate that the circuitry works when it receives sufficient power. We will continue to prepare more of these devices in the coming months for possible in-vivo testing by a number of our collaborators.

Finally, during the past quarter we designed and simulated the complete circuitry for a fully integrated 8-channel mini-microstimulator that can operate using on-chip coils. This circuitry can be used for peripheral nerve stimulation applications and can deliver current pulses to any of 8 electrodes. The circuitry has been fully simulated and is being laid out. A mask set will be generated within the next month and fabrication will proceed shortly afterwards. We also further characterized on-chip coils for power and data reception and are confident that sufficient levels of power can be transmitted to these on-chip coils for peripheral nerve applications. The mini-microstimulator can thus operate without the need for any hybrid components, which will make the fabrication and assembly of these systems much easier.

1. INTRODUCTION

This project deals with the development of hermetic, biocompatible micropackages and feedthroughs for use in a variety of implantable neural prostheses for sensory and motor handicapped individuals. The project also aims at continuing work on the development of a telemetrically powered and controlled neuromuscular microstimulator for functional electrical stimulation. The primary objectives of the project are: 1) the development and characterization of hermetic packages for miniature, silicon-based, implantable three-dimensional structures designed to interface with the nervous system for periods of up to 40 years; 2) the development of techniques for providing multiple sealed feedthroughs for the hermetic package; 3) the development of custom-designed packages and systems used in chronic stimulation or recording in the central or peripheral nervous systems in collaboration and cooperation with groups actively involved in developing such systems; and 4) establishing the functionality and biocompatibility of these custom-designed packages in *in-vivo* applications. Although the project is focused on the development of the packages and feedthroughs, it also aims at the development of inductively powered systems that can be used in many implantable recording/stimulation devices in general, and of multichannel microstimulators for functional neuromuscular stimulation in particular.

Our group here at the Center for Integrated Sensors and Circuits at the University of Michigan has been involved in the development of silicon-based multichannel recording and stimulating microprobes for use in the central and peripheral nervous systems. More specifically, during the past two contract periods dealing with the development of a single-channel inductively powered microstimulator, our research and development program has made considerable progress in a number of areas related to the above goals. A hermetic packaging technique based on electrostatic bonding of a custom-made glass capsule and a supporting silicon substrate has been developed and has been shown to be hermetic for a period of at least a few years in salt water environments. This technique allows the transfer of multiple interconnect leads between electronic circuitry and hybrid components located in the sealed interior of the capsule and electrodes located outside of the capsule. The glass capsule can be fabricated using a variety of materials and can be made to have arbitrary dimensions as small as 1.8mm in diameter. A multiple sealed feedthrough technology has been developed that allows the transfer of electrical signals through polysilicon conductor lines located on a silicon support substrate. Many feedthroughs can be fabricated in a small area. The packaging and feedthrough techniques utilize biocompatible materials and can be integrated with a variety of micromachined silicon structures.

The general requirements of the hermetic packages and feedthroughs to be developed under this project are summarized in Table 1. Under this project we will concentrate our efforts to satisfy these requirements and to achieve the goals outlined above. There are a variety of neural prostheses used in different applications, each having different requirements for the package, the feedthroughs, and the particular system application. The overall goal of the program is to develop a miniature hermetic package that can seal a variety of electronic components such as capacitors and coils, and integrated circuits and sensors (in particular electrodes) used in neural prostheses. Although the applications are different, it is possible to identify a number of common requirements in all of these applications in addition to those requirements listed in Table 1. The packaging and feedthrough technology should be capable of:

1- protecting non-planar electronic components such as capacitors and coils, which typically have large dimensions of about a few millimeters, without damaging them;
2- protecting circuit chips that are either integrated monolithically or attached in a hybrid fashion with the substrate that supports the sensors used in the implant;
3- interfacing with structures that contain either thin-film silicon microelectrodes or conventional microelectrodes that are attached to the structure;

Table 1: General Requirements for Miniature Hermetic Packages and Feedthroughs for Neural Prostheses Applications

Package Lifetime:
≥ 40 Years in Biological Environments @ 37°C

Packaging Temperature:
≤360°C

Package Volume:
10-100 cubic millimeters

Package Material:
Biocompatible
Transparent to Light
Transparent to RF Signals

Package Technology:
Batch Manufactureable

Package Testability:
Capable of Remote Monitoring
In-Situ Sensors (Humidity & Others)

Feedthroughs:
At Least 12 with ≤125μm Pitch
Compatible with Integrated or Hybrid Microelectrodes
Sealed Against Leakage

Testing Protocols:
In-Vitro Under Accelerated Conditions
In-Vivo in Chronic Recording/Stimulation Applications

We have identified two general categories of packages that need to be developed for implantable neural prostheses. The first deals with those systems that contain large components like capacitors, coils, and perhaps hybrid integrated circuit chips. The second deals with those systems that contain only integrated circuit chips that are either integrated in the substrate or are attached in a hybrid fashion to the system.

Figure 1 shows our general proposed approach for the package required in the first category. This figure shows top and cross-sectional views of our proposed approach here. The package is a glass capsule that is electrostatically sealed to a support silicon substrate. Inside the glass capsule are housed all of the necessary components for the system. The electronic circuitry needed for any analog or digital circuit functions is either fabricated on a separate circuit chip that is hybrid mounted on the silicon substrate and electrically connected to the silicon substrate, or integrated monolithically in the support silicon substrate itself. The attachment of the hybrid IC chip to the silicon substrate can be performed using a number of different technologies such as simple wire bonding between pads located on each substrate, or using more sophisticated techniques such as flip-chip solder reflow or tab bonding. The larger capacitor or microcoil components are mounted on either the substrate or the IC chip using appropriate epoxies or solders. This completes the assembly of the electronic components of the system and it should be possible to test the system electronically at this point before the package is completed. After testing, the system is packaged by placing the glass capsule over the entire system and bonding it to the silicon substrate using an electrostatic sealing process. The cavity inside the glass package is now hermetically sealed against the outside environment. Feedthroughs to the outside world are provided using the grid-feedthrough technique discussed in previous reports. These feedthroughs transfer the electrical signals between the electronics inside the package and various elements outside of the package. If the package has to interface with conventional microelectrodes, these microelectrodes can be attached to bonding pads located outside of the package; the bond junctions will have to be protected from the external environment using various polymeric encapsulants. If the package has to interface with on-chip electrodes, it can do so by integrating the electrode on the silicon support substrate. Interconnection is simply achieved using on-chip polysilicon conductors that make the feedthroughs themselves. If the package has to interface with remotely located recording or stimulating electrodes that are attached to the package using a silicon ribbon cable, it can do so by integrating the cable and the electrodes again with the silicon support substrate that houses the package and the electronic components within it.

Figure 2 shows our proposed approach to package development for the second category of applications. In these applications, there are no large components such as capacitors and coils. The only component that needs to be hermetically protected is the electronic circuitry. This circuitry is either monolithically fabricated in the silicon substrate that supports the electrodes (similar to the active multichannel probes being developed by the Michigan group), or is hybrid attached to the silicon substrate that supports the electrodes (like the passive probes being developed by the Michigan group). In both of these cases the package is again another glass capsule that is electrostatically sealed to the silicon substrate. Notice that in this case, the glass package need not be a high profile capsule, but rather it need only have a cavity that is deep enough to allow for the silicon chip to reside within it. Note that although the silicon IC chip is originally 500μm thick, it can be thinned down to about 100μm, or can be recessed in a cavity created in the silicon substrate itself. In either case, the recess in the glass is less than 100μm deep (as opposed to several millimeters for the glass capsule). Such a glass package can be easily fabricated in a batch process from a larger glass wafer.
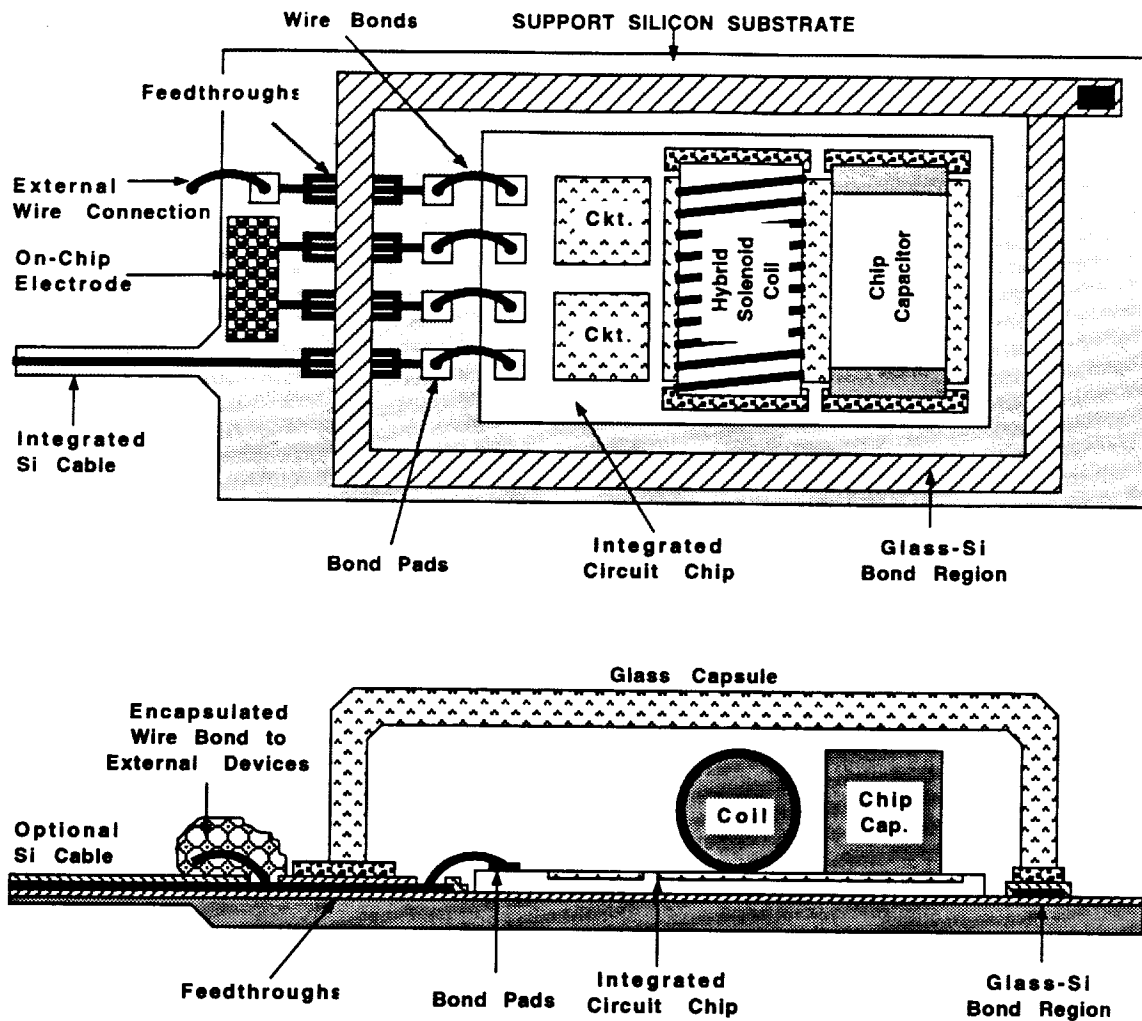
Figure 1: A generic approach for packaging implantable neural prostheses that contain a variety of components such as chip capacitors, microcoils, and integrated circuit chips. This packaging approach allows for connecting to a variety of electrodes.

We believe the above two approaches address the needs for most implantable neural prostheses. Note that both of these techniques utilize a silicon substrate as the supporting base, and are not directly applicable to structures that use other materials such as ceramics or metals. Although this may seem a limitation at first, we believe that the use of silicon is, in fact, an advantage because it provides several benefits. First, it is biocompatible and has been used extensively in biological applications. Second, there is a great deal of effort in the IC industry in the development of multi-chip modules (MCMs), and many of these efforts use silicon supports because of the ability to form high density interconnections on silicon using standard IC fabrication techniques. Third, many present and future implantable probes are based on silicon micromachining technology; the use of our proposed packaging technology is inherently compatible with most of these probes, which simplifies the overall structure and reduces its size.

Once the above packages are developed, we will test them in biological environments by designing packages for specific applications. One of these applications is in recording neural activity from cortex using silicon microprobes developed by the Michigan group under separate contracts. The other involves the chronic stimulation of muscular tissue using a multichannel microstimulator for the stimulation of the paralyzed larynx. This application has been developed at Vanderbilt University. Once the device is built, it will be used by our colleagues at Vanderbilt to perform both biocompatibility tests and functional tests to determine package integrity and suitability and device functionality for the reanimation of the paralyzed larynx. The details of this application will be discussed in future progress reports.
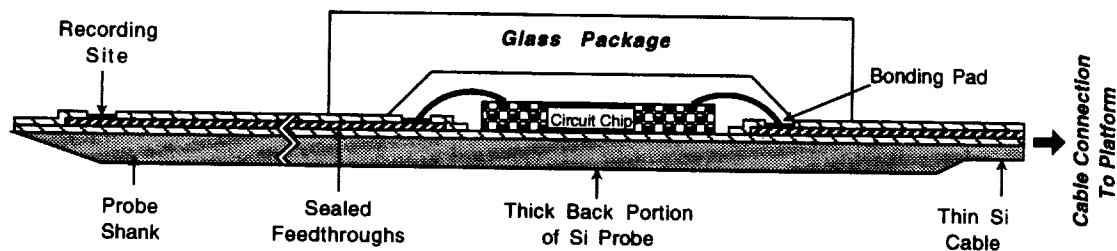

Figure 2: Proposed packaging approach for implantable neural prostheses that contain electronic circuitry, either monolithically fabricated in the probe substrate or hybrid attached to the silicon substrate containing microelectrodes.

2. ACTIVITIES DURING PAST QUARTER

2.1 Hermetic Packaging

Over the past few years we have developed a bio-compatible hermetic package with high density, multiple feedthroughs. This technology utilizes electrostatic bonding of a custom-made glass capsule to a silicon substrate to form a hermetically sealed cavity, as shown in Figure 3. Feedthrough lines are obtained by forming closely spaced polysilicon lines and planarizing them with LTO and PSG. The PSG is reflowed at 1100° C for 2 hours to form a planarized surface. A passivation layer of oxide/nitride/oxide is then deposited on top to prevent direct exposure of PSG to moisture. A layer of fine-grain polysilicon (surface roughness 50Å rms) is deposited and doped to act as the bonding surface. Finally, a glass capsule is bonded to this top polysilicon layer by applying a voltage of 2000V between the two for 10 minutes at 320 to 340° C, a temperature compatible with most hybrid components. The glass capsule can be either custom molded from Corning code #7740 glass, or can be batch fabricated using ultrasonic micromachining of #7740 glass wafers.
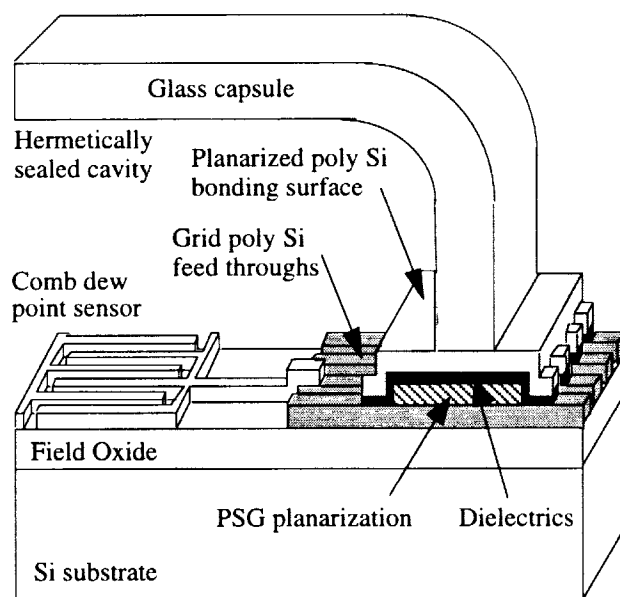
Figure 3: The structure of the hermetic package with grid feedthroughs.

During the past few years we have electrostatically bonded and soak tested over one hundred and sixty of these packages. The packages successfully prevent leakage in soak tests at 95° C for over 4 months on average and at 85° C for over 16 months in deionized water. The bonding yield has varied between 85% to 72% (yield is defined as the percentage of packages which last more than 24 hours soaking in DI water). It should be mentioned that the earlier tests that have been going for more than about 2 years (room temperature soak tests in saline and the 85° C and the 95° C tests in deionized water) have been made with silicon substrates that are thinned(~150μm) and bonded to the custom made glass capsules. The relatively recent tests (85° C and 95° C tests in saline) are performed with the silicon substrates having full thickness(~500μm) and bonded to the ultrasonically machined glass capsules with a flat top surface. By creating recesses in a glass wafer, it is also possible to make a low profile package with a smaller cavity that could be used to encapsulate integrated circuit chips. We have performed soak tests both with deionized water and phosphate buffered saline during the past year. Due to the enhanced dissolution rate of polysilicon in saline, the samples in saline have been concluded. We currently

have devices being tested in deionized water for over 2.5 years at 85° C. The in-vivo test results from both the normal package and the smaller package reveal that the devices are biocompatible and rugged. We have also started to characterize the mechanical strength of this glass-silicon package, as will be reported below.

2.1.1 Ongoing Accelerated Soak Tests in Deionized Water

We have continued our accelerated soak tests during this quarter. At the present time, out of the original 20 packages we have 4 packages that have lasted for more than two and a half years of testing time with no sign of moisture penetration inside them. In these tests temperature is chosen as the accelerating factor since it is easy to control and also the diffusion of moisture is a strong (exponential) function of temperature. We had started soaking 10 samples each at 85° C and 95° C. Tables 2 and 3 below list some pertinent data from these soak tests. Figure 4 summarizes the final results from the 95° C soak tests and Figure 5 summarizes the results so far from the 85° C tests. These figures also list the causes of failure for individual packages when it is known, and they show a curve fit to our lifetime data to illustrate the general trend. The curve fit, however, only approximates the actual package lifetimes since some of our packages failed due to breaking during testing rather than due to leakage.

At the beginning of this quarter, we had 4 packages soaking at 85°C. These packages are still dry and under test. For these packages we define failure as the room temperature condensation of moisture inside the package. The testing sequence for these packages starts by cooling the sample to room temperature from its soak bath at the elevated temperature. The samples are next rinsed with deionized water and then dried with a nitrogen gun. We then measure the impedance of the dew point sensors and inspect the sample carefully for leakage under the microscope. The significant change in impedance (about 2 orders of magnitude) and observation of visible condensation inside the package would both be classified as the failure of the package under test. Of the original 10 samples in the 95°C tests, the longest lasting package survived for a total of 484 days. The calculated mean time to failure of these packages are 135.7 days excluding the handling errors. Of the original 10 packages in the 85° C soak tests there are still 4 with no sign of room temperature condensation. The longest lasting package in the 85° C tests has lasted a total of 961 days and is still under test. The worst case mean time to failure for these tests has been calculated as 760 days excluding the handling errors. We are currently conducting tests to stop the dissolution of polysilicon in saline solution and would shortly start a new set of soak tests in the coming quarter.

2.1.2 Interpretation of the Long Term Soak Testing Results in Deionized Water

Generally during accelerated testing, one models the mean time to failure (MTTF) as an Arrhenius processes (In the VLSI industry this model is used for failure due to diffusion, corrosion, mechanical stress, electromigration, contact failure, dielectric breakdown, and mobile ion/surface inversion). The generalized equation use in all these cases is given below where MTTF is the mean time to failure, A is a constant, ξ is the stress factor other than temperature, (such as pressure or relative humidity), n is the stress dependence, Q is the activation energy, K_B is Boltzman's constant, and T is the temperature in Kelvin.

$$MTTF = A \cdot \xi^{-n} \cdot e^{\left(\frac{Q}{K_B T}\right)}$$

Table 2: Key data for 95°C soak tests in DI water.

Number of packages in this study	10
Soaking solution	DI water
Failed within 24 hours (not included in MTTF)	1
Packages lost due to mishandling	2
Longest lasting packages in this study	484 days
Packages still under tests with no measurable room temperature condensation inside	0
Average lifetime to date (MTTF) including losses attributed to mishandling	*118.7 days*
Average lifetime to date (MTTF) not including losses attributed to mishandling	*135.7 days*

Table 3: Key data for 85°C soak tests in DI water.

|	
Number of packages in this study	10
Soaking solution	DI water
Failed within 24 hours (not included in MTTF)	2
Packages lost due to mishandling	3
Longest lasting packages so far in this study	961 days
Packages still under tests with no measurable room temperature condensation inside	4
Average lifetime to date (MTTF) including losses attributed to mishandling	*484.9 days*
Average lifetime to date (MTTF) not including losses attributed to mishandling	*760 days*
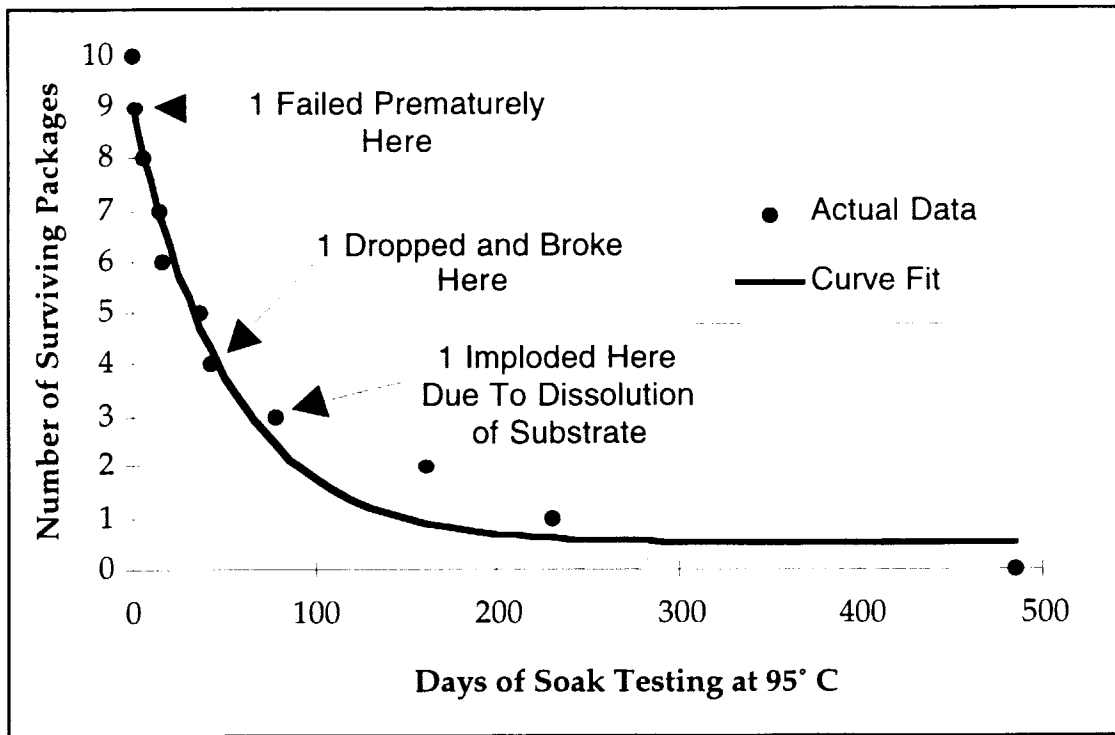
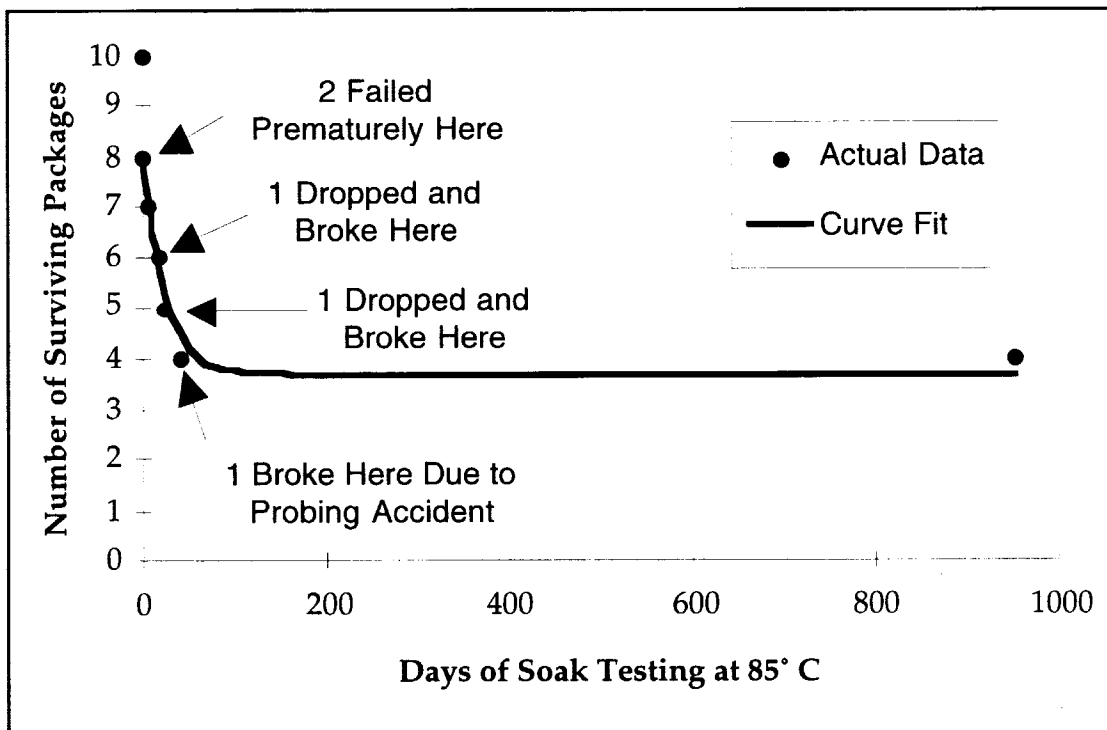Figure 4: Summary of the lifetimes of the 10 packages which have been soak tested at 95° C in DI water.

Figure 5: Summary of the lifetimes of the 10 packages which have been soak tested at 85° C in DI water.

For the accelerated soak tests that we have performed on the packages, there was no stressing factor other than temperature, so the ξ term drops out of the above equation. The resulting equation can be rewritten as a ratio of MTTFs as it is below. This is the model we are using to interpret the accelerated soak tests performed during the past year.

$$AF = \frac{MTTF_{Normal}}{MTTF_{Accelerated}} = e^{\frac{Q}{K_B}\left(\frac{1}{T_{Normal}} - \frac{1}{T_{Accelerated}}\right)}$$

By using the current MTTFs at 85° C and 95° C, we can easily calculate the activation energy (Q) and from this activation energy we can proceed to obtain an acceleration factor (AF) for these tests, and then calculate the MTTF at body temperature. Moreover, after analyzing our failed samples we have found out and mentioned in the past progress reports that some of the samples at the 95°C tests have failed prematurely due to enhanced dissolution rate for silicon at this temperature. Since the dissolution reaction is an exponential function of temperature, the samples at the 85° C tests have been effected less than the ones at 95°C. The model we use only accounts for acceleration of moisture diffusion, but not dissolution. We still keep and update the data for the tests in 85° C tests. Moreover, for our calculations we assume that all the samples in the 85° C tests have also failed the same time as the longest going sample in the 95° C tests and make the calculations as follows:

$$MTTF\big|_{85°C} = 257.6\,Days \qquad MTTF\big|_{95°C} = 118.7\,Days$$

Q=0.88 eV, AF(95°C)=179.5, AF(85°C)=82.7

$$MTTF\big|_{37°C} = 58.4\,Years$$

This is admittedly a very conservative figure because it discounts the longer mean time to failure of the packages being soaked at 85°C. We should also note that we have included every single sample in the 85° C and 95° C soak tests in this calculation except the 15% which failed during the first day (we assume that these early failures can be screened for). Moreover, some of these capsules have failed due to mishandling during testing rather than due to actual leakage of the package. If we disregard the samples that we have attributed failure to mishandling we obtain a longer mean time to failure:

$$MTTF\big|_{85°C} = 396\,Days \qquad MTTF\big|_{95°C} = 136\,Days$$

Q=1.217 eV, AF(95°C)=1304, AF(85°C)=447

$$MTTF\big|_{37°C} = 485\,Years$$

Both of these values indicate that indeed these packages last for many decades in aqueous environments and provide the protection needed for implantable systems.

2.1.3 Ongoing Room Temperature Soak Tests in Saline

We have been soaking a group of packages in phosphate buffered saline at room temperature for the past 2 and a half years. Table 4 below lists some of the pertinent data from these soak tests. These tests have been started for two main reasons. First, we wanted to have some soak tests in saline and since at higher temperatures we were getting dissolution of silicon in saline, at this temperature we hoped to obtain data without any significant dissolution. Second, we wanted to have some soak data independent of the acceleration technique used. To obtain meaningful data from these tests may take a long time, however the samples in these tests would act as a control group for our accelerated tests.

We started with 6 packages soaking in saline at room temperature. One of these packages failed within one day, most likely due to surface defects or poor bonding due to misalignment. Another one failed after 160 days of soaking. The remaining 4 samples are dry and still under test. These samples, similar to our other samples, are tested visually with the aid of a microscope and electrically with the help of dew point sensors integrated into the package substrate. The longest lasting sample in these tests has reached a total of 863 days and is still under test. We have calculated a worst case mean time to failure of 716 days.

Table 4: Data for room temperature soak tests in saline.

Number of packages in this study	6
Soaking solution	Saline
Failed within 24 hours (not included in MTTF)	1
Packages lost due to mishandling	1
Longest lasting packages in this study	863 days
Packages still under tests with no measurable room temperature condensation inside	4
Average lifetime to date (MTTF)	*715.6 days*

2.1.4 Bond Strength Measurements For the Microstimulator Package

In previous progress reports we had indicated that the strength of the silicon-glass bond exceeded the fracture strength of the glass or silicon substrates. This was confirmed by breaking the bond and observing that fracture occurred in the glass and not where the bond was formed. In order to obtain a quantitative measure of the strength of the bond, we have initiated a series of new experiments. Although these initial experiments are somewhat crude, they have helped us determine the approximate bond strength for these glass-silicon packages. Several packages have been prepared using the original microstimulator silicon substrate and a glass capsule. Accordingly, these devices are identical to the actual microstimulator devices. in order to be able to attach a large load to the glass and silicon pieces, we next glued a piece of wood block to silicon and glass side of the device as a support and a handle using a household adhesive. Figure 6 below shows a drawing of the setup. One end of the device is held fixed whereas weights are gradually added to the other end until the package is broken apart. The results of the experiments are summarized in Table 5 below. These values were calculated by dividing the total load applied by the bonded area between the glass and silicon. The bond strengths measured were in the range 3-9

MPa range. These values are consistent with what other investigators have reported in the literature for bond strength of typical glass-silicon anodic bonds. We should also mention that the maximum applied pressure of 8.9 MPa corresponds to about 11 pounds. When the bond breaks we observe that in almost all of the samples the break typically occurs in the glass capsule region of the package.

Figure 7 shows SEM micrographs of one of these broken packages. Note that it is indeed the glass package that breaks, and that the bond has a higher fracture limit than either silicon or glass. A close-up view of the bond region shows the corner of the bond area, where one can easily see remnants of the glass package still bonded to the silicon substrate. We should also note that among all the samples tested none of the fractures occurred in the glass to silicon interface indicating the strength of the glass to silicon anodic bonds. In summary, the devices can resist large tensile forces which would appear both during the implant and also inside the body. We hope to perform more tests to further characterize the strength of our glass to silicon package.
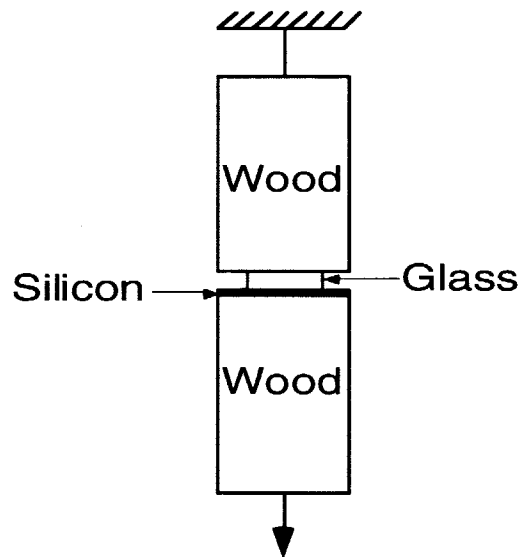

Figure 6: The set-up for the tensile pull tests.

Table 5: Summary of pull test results.

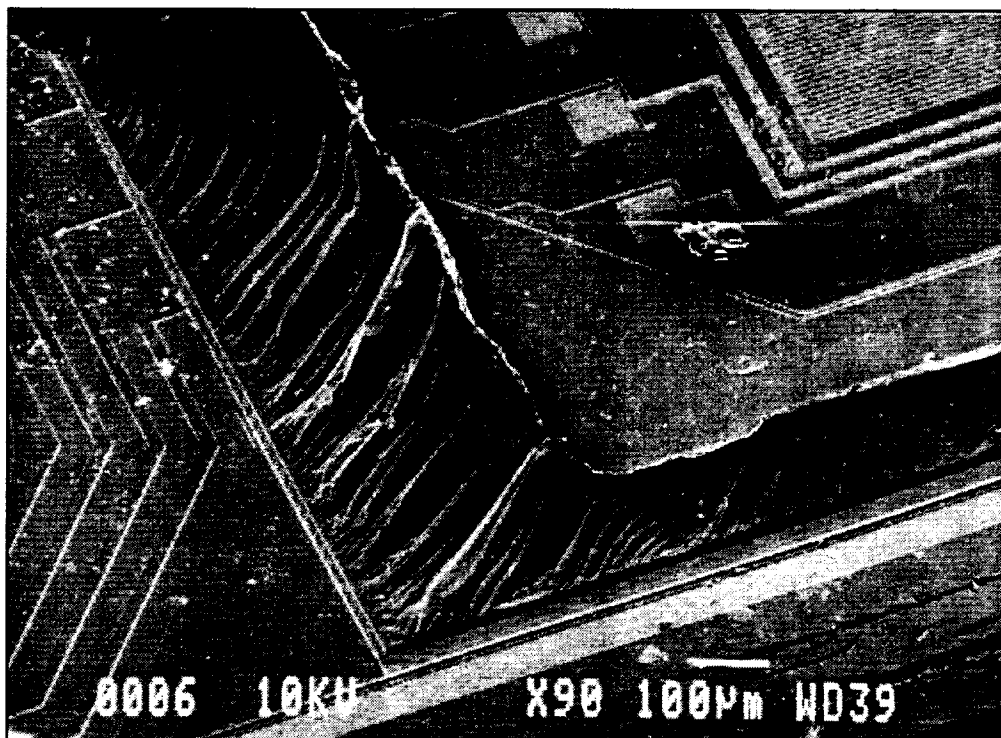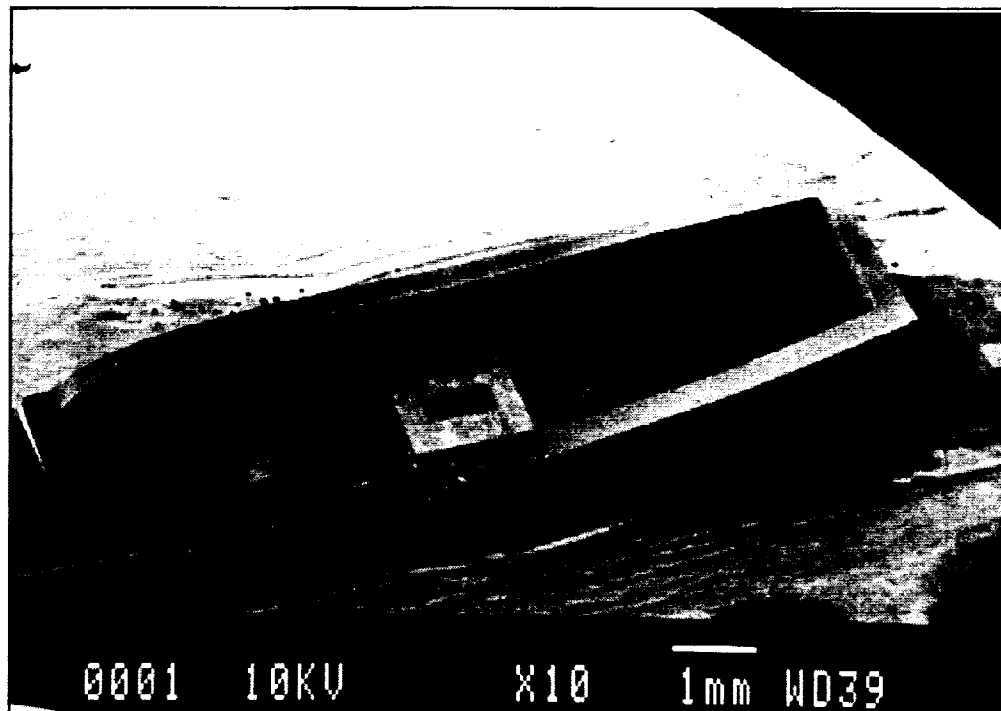| Sample Number	Average Tensile Strength [MPa]
14	4.8
15	7.9
16	8.9
20	3.2
21	4.8
23	5.4

Figure 7: SEM micrographs of the silicon-glass package after fracture. In the close-up view one can easily see glass remnants on top of the bond regions indicating the higher fracture limit of the glass-silicon bond.

2.1.5 In-Vivo Tests

In past progress reports, we reported that several low profile devices were fabricated and sent to Dr. Humayun at Johns Hopkins University. These devices were made by recessing a glass wafer where needed, dicing the glass wafer, and then bonding the glass pieces to a silicon substrate. The main difference between this and a standard microstimulator is that the entire device is less than a millimeter in height. Due to space limitations the electrodes from the devices have been diced prior to implantation so that the length of the device is less than 10 mm. The group at Johns Hopkins has had 2 of our devices implanted into the eye in 2 rabbits. The device that has been implanted for a month has been already explanted. This device was floating in the fluid in the eye and not in contact with tissue for the implant duration. We are told that the second device would be implanted for a period of 3 months. The tests results from these recent tests are still not available, and will be provided in the next progress report. We are also preparing several passive devices that could be tested for biocompatibility by Dr. Lisa Reidy at the Hines VA Hospital, Illinois. The biocompatibility tests that have been performed so far in different tissues at the various institutions (rat dura: University of Michigan, bladder: Hines VA hospital, rat dorsum: Vanderbilt University, and rabbit eye: Johns Hopkins Univ.) all indicate that for the duration of the tests (ranging from one month to one year), the packages are biocompatible and provide protection against attack by body fluids. We hope to continue these tests and provide additional data on these results.

2.2 Status Of Microstimulator Circuitry

This past quarter we continued to test the microstimulator chips from the latest CMOS fabrication run. We are narrowing down the possibilities that may explain the large leakage currents observed in these chips. Two main suspicions are contaminated field oxide and parasitic devices that may possibly be turning on under certain circumstances. Although we continued our testing of these chips during the past quarter, we have not yet been able to pinpoint the problem. We have made some changes to our layout to eliminate any possibility of leakage paths, however, in spite of these changes we still cannot explicitly explain the reasons for the higher leakage currents in the chips we fabricated last year. we will continue testing of these chips and we will hopefully find the source of problem. However, it is possible that the higher leakage current was due to a problem in processing which cannot be determined by testing of the devices on the chips. If this is the case, then our only hope will be to refabricate the wafers and see what the new run will produce in terms of test results. It should be noted that alongside the microstimulator circuitry, we had also fabricated other circuitry which had been fabricated in our facility in the past and had worked perfectly. However, this same circuitry showed a higher leakage than expected on the microstimulator fabrication run. We will continue our testing of these chips and will report on any new findings in the next progress report.

Since these chips have consistently had high leakage currents, we have been unable to use them to assemble working microstimulators. However, we have on reserve many chips from the previous CMOS run. These consume about 50% higher currents than the present generation was intended to use, as modeled in simulations (additionally, the new generation was designed to have a steadier output current with hard-programmable amplitude, through laser cuts.) This higher current draw made it necessary to change our assembly approach somewhat. To compensate for the higher power consumption of these older but fully working chips, we must use slightly larger receiver coils, about 2mm instead of 1.3mm diameter. To a first order approximation, this enables us to receive roughly 2-2.4 times the power through the telemetric link. Since these larger coils do not fit within the present glass capsules (indeed, a new electrode substrate would be necessary to accommodate the larger glass capsules needed), we decided to encapsulate microstimulator systems in silicone rubber.

Because no high temperature assembly steps were used, it was possible to reinforce leads (both bonding leads and microwelded receiver coil leads) with silastic and Type A medical grade, single component silicone rubber. In glass encapsulated units, nonconductive polyimide would be used. After attaching and welding the charge storage capacitor and receiver coil carefully and reinforcing the leads, the chip with hybrid components was attached and bonded to an electrode substrate. Then the whole assembly was attached and bonded to a test and electrode activation stalk. Finally this assembled unit was encapsulated in silicone, first packing the space around the bonding wires for strength and to eliminate voids, and then continuing with the rest of the unit (being very careful not to smear any silicone on the electrodes). This last step was particularly challenging with the present electrode substrate design, since the space between the bonding wires and the electrodes is quite small.

We prepared a few such devices for our colleagues from Hines Veterans Affairs Medical Research Center. Although some of these units became damaged in assembly, the others worked well under telemetric tests using a 9cm diameter transmitter coil. The output stimulus current was measured to be about 10mA as expected. Its magnitude, as documented in previous reports, was somewhat dependent on received voltage and thus on position within the transmitter coil. The devices showed a large tolerance to misalignment within the receiver coil (roughly 40-50° off center axis), since the logic continues to work well even at lower received voltages.

However, these devices were not delivered for *in vitro* and eventual *in vivo* testing at Hines because a couple of observations indicate that it would be beneficial to modify the electrode substrate currently used. For many applications, it is useful to have the electrodes spaced further apart, on the order of two or three centimeters instead of 1cm as in the present design. Such is certainly the case for the intended use at Hines, which is to stimulate the colon to induce a natural peristaltic motion. Furthermore it would be immensely useful to have the electrodes rest on a flexible substrate that can conform more effectively to the contours of the biological region being stimulated. Additionally, methods for fabricating the electrodes on the back side of the electrode substrate should be considered, or other methods devised to ensure that the contact area is maximized between the electrodes and the target organ. All of these considerations are equally valid in the design of multichannel electrode substrates. Longer electrode substrates would also have the advantage of giving more room to encapsulate the microstimulator in silicone without worrying about harming bonds or accidentally smearing the electrodes. This is an issue of importance while we continue encapsulating units in silicone, until the leakage problems are resolved with the present generation design and until we have a new CMOS run of microstimulator devices. Otherwise, not only may yield be affected but also the hermeticity of the devices and hence their long term durability when implanted. Of course, longer electrode substrates introduce challenges of their own: processing the substrate to provide flexibility for the electrode portion along with structural support for the chip and hybrid components, reducing the electrode access resistance so that strong stimulus currents can be delivered without increasing compliance voltages on the chip, etc. We have begun to investigate these options but have not yet decided upon or fabricated any prototypes.

2.3 Packaging and Microtelemetry For Next Generation Microstimulators

The single-channel microstimulator that has been under development for the past few years under funding from the Neural Prosthesis Program, is about 3 orders of magnitude smaller than conventional implantable stimulation units that use hybrid thin-film technology. As part of our contract goals, we are required to develop miniature packages for a variety of implantable neural prostheses. In order to minimize the size of these packages, we have been examining ways to reduce the volume of implantable stimulators by another order of magnitude. Figure 8 illustrates how this drastic size reduction can be achieved. By far the largest components .in the

microstimulator system are the charge storage capacitor and the discrete receiver coil. These two components take up about 90% of the total microstimulator volume. As shown in Fig. 8, the volume of the microstimulator can be reduced by an order of magnitude by integrating the receiver coil directly on the CMOS substrate and by not using a charge storage capacitor. While the microstimulator is currently about 2.5 mm thick and has a volume of about 50 mm³, a system with an integrated coil and no charge storage capacitor will be in the 300 μm to 500 μm thickness range and will have a volume of about 6 mm³. We call these extremely low volume FES systems mini-microstimulators.
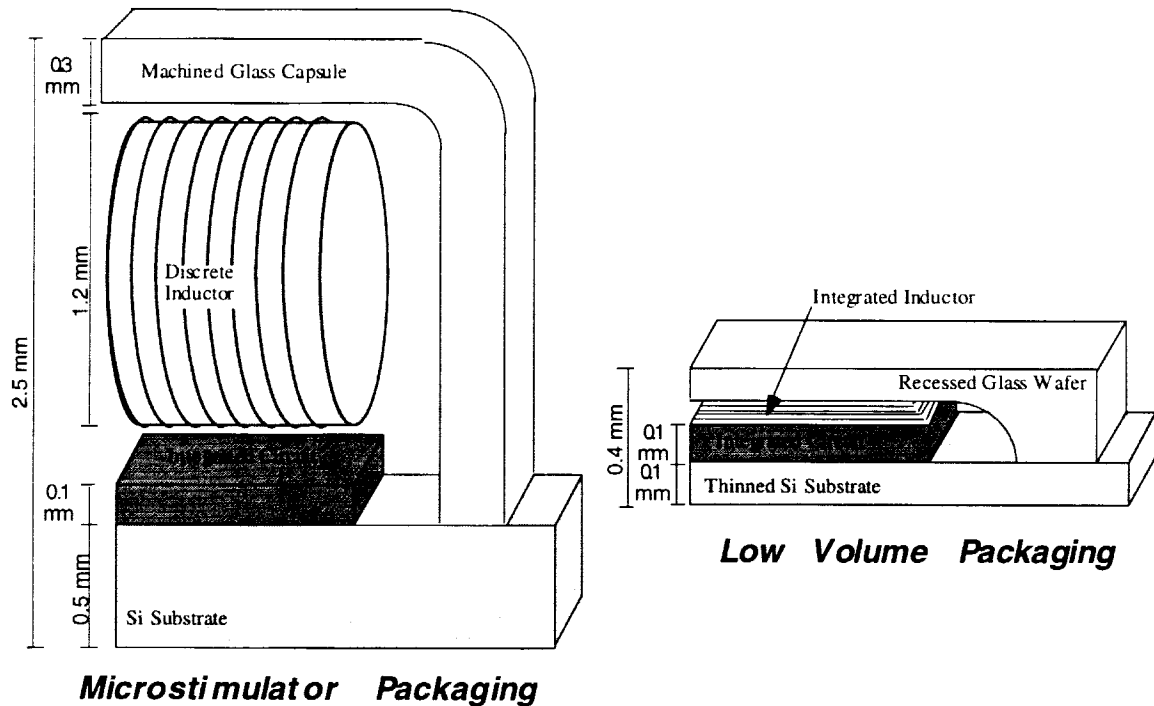

Figure 8: A scale drawing comparing the volume of the microstimulator with the volume of a mini-microstimulator.

We are developing a nerve cuff stimulation system to demonstrate the feasibility of a telemetry powered mini-microstimulator. Stimulating nerve cuffs are a well suited application for a mini-microstimulation device because they need relatively low current levels. Typical nerve cuff stimulation levels are 100 μA to 2 mA, which is a good fit with the 3 mA output that is feasible using on-chip coils and no charge storage capacitor (for comparison the microstimulator stimulates with an output current of 10 mA or more). Figure 9 shows a photograph of some of the on-chip receiver coils that we have fabricated and tested, and Figure 10 shows one of these coils with integrated RF receiver circuitry mounted on top of it for testing. This circuitry includes a 4 MHz tuned RF receiver, a supply generator, a clock recovery circuit, and a data demodulator. The coils and RF receiver circuit have been successfully tested telemetrically. Although for this initial study the circuitry and the coil were fabricated on separate silicon substrates and hybrid attached, the coil technology is fully CMOS compatible, and in the future they will be fabricated together. Table 6 summarizes the specifications for the full 8-channel nerve cuff system which we are developing, and Figure 11 shows an exploded view of such a system. Note that the nerve cuff and electrodes can be either integrated directly with the hermetic packaging substrate, or the nerve cuff could be attached by a connector.
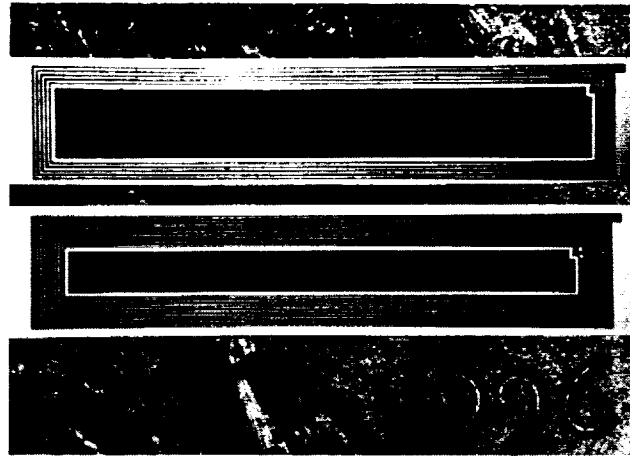
17

Figure 9: Photograph of 5 and 10 turn Cu on-chip coils with NiFe cores. These coils are 2 by 10 mm.
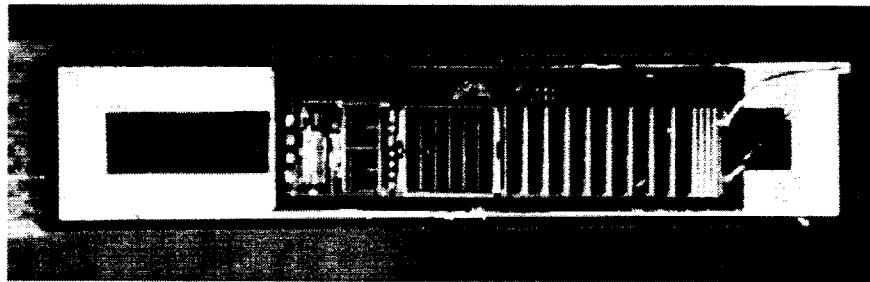

Figure 10: Photograph of the integrated RF receiver circuitry mounted on top of a 10 turn on-chip coil. This 1.29 by 5.78 mm circuit includes a 4 volt generator, a data demodulator, and a clock recovery circuit.

Table 6: The specifications for a telemetry powered stimulating nerve cuff.

8-Channel Peripheral Nerve Stimulation System Specifications

General

Dimensions = 2.0 mm X 10 mm X 0.5 mm	Power Delivery = Telemetry
Power Consumption < 15 mW	On Chip Regulated Supply = 4 Volts, Gnd

Telemetry Link

Receiver Coil = On-chip (2.2mm X 10mm)	Range = 3 cm
Transmitter Coil = Planar, air core (80 mm dia.)	Carrier Frequency = 4 MHz
Modulation Frequency = 1 kHz to 50 kHz	

Stimulation

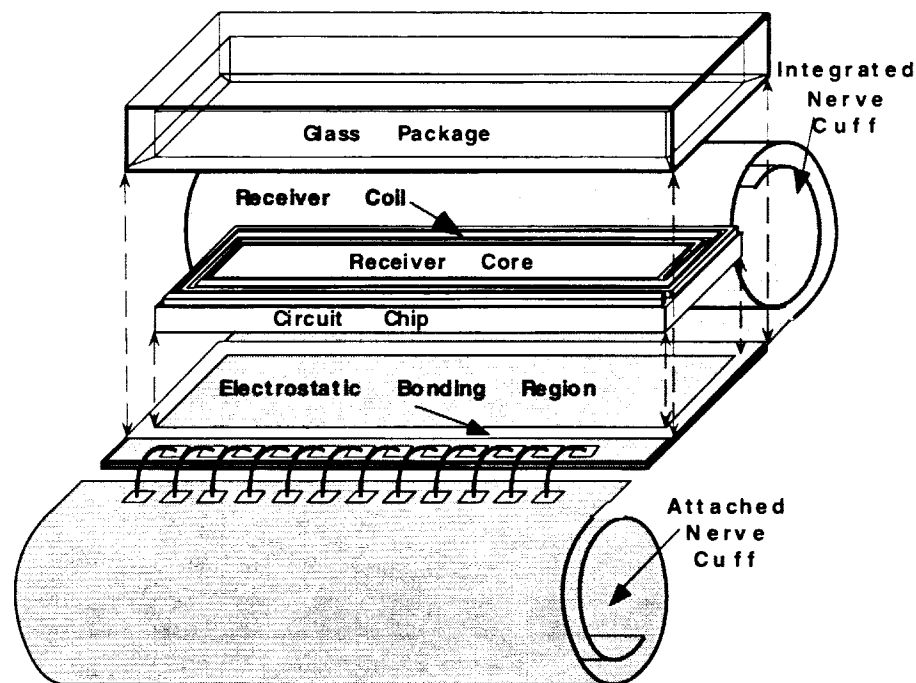|	
Output Channels = 8	Amplitude = 0 to 2 mA (62.5 μA steps)
Duration = 0 to 2047 μS (2 μS steps)	Stimulation Protocol = Bi-phasic
Frequency $\leq$ 50 Hz	Output Load < 1.5 KΩ

18

Figure 11: One mini-microstimulator application is this nerve cuff. The nerve cuff can be either integrated directly with the packaging substrate, or attached by a connector.

This quarter we designed and exhaustively simulated the full 8-channel peripheral nerve stimulation system circuitry. We will layout and fabricate this circuitry during the coming quarter.

2.3.1 Design of Full System Circuitry

This quarter the circuitry for a full 8-channel nerve cuff was designed and fully simulated. This circuitry contains 2,710 transistors, making it only slightly smaller than the multi-channel microstimulator, which contains 2,800 transistors (For comparison, the single channel microstimulator contains about 1,200 transistors). Although this circuitry has not yet been physically laid out, we estimate that it will easily fit in a 2mm by 10mm die (this is the dimensions of the on-chip coils that we have been testing). The circuitry is designed to consume 3.5 mW of power when not stimulating, and a maximum of 13.5 mW of power during maximum stimulation. For comparison, the single channel microstimulator was designed to consume 50 mW. Much of this power saving in the mini-microstimulator is due to the fact that the mini-microstimulator runs on a single 4V supply, while the microstimulator requires both a 4V and 8V supply. Other power savings come from lower current consumption of the analog circuit blocks and lowering the system clock to 500 kHz.

A block diagram for the entire system circuitry is shown in Figure 12. The largest block of the mini-microstimulator's circuitry is the digital control logic, which contains 2,300 of the system's 2,710 transistors. A block diagram of the digital circuitry is shown in Figure 13.
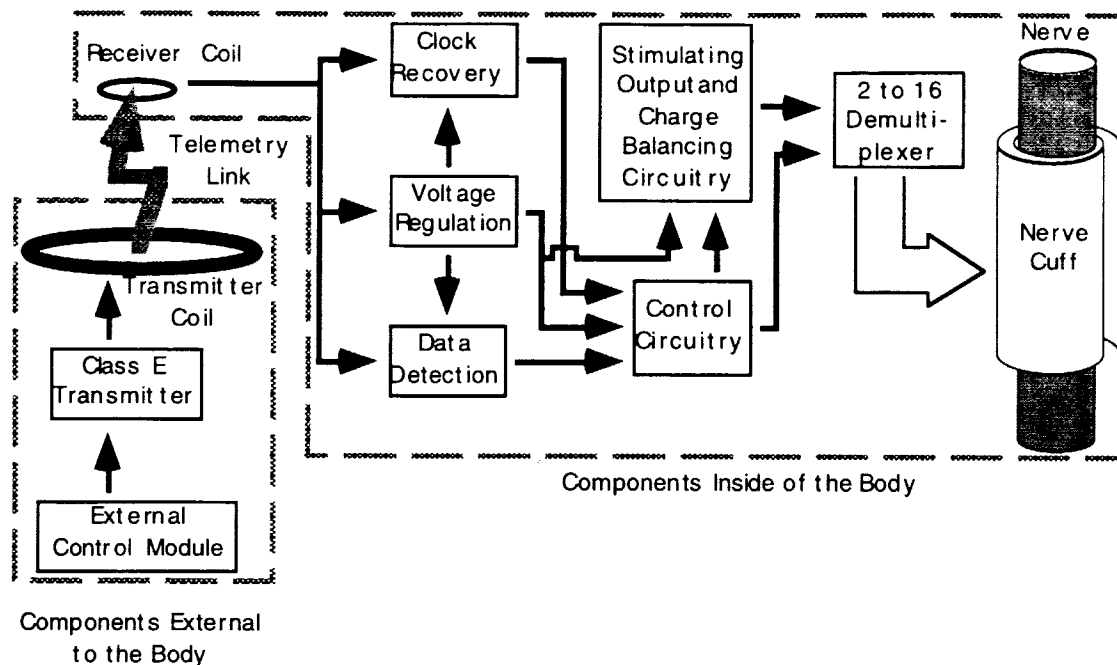
19

Figure 12: Block diagram of a telemetrically powered/controlled peripheral stimulation system.

2.3.2 Data Transmission Scheme

Before the mini-microstimulator's control logic could be designed, the data transmission scheme had to be determined. The mini-microstimulator will use a very similar pulse width modulated, amplitude shift key encoded data transmission scheme as the microstimulator. One difference is that the mini-microstimulator will use a 4 MHz carrier rather than the 2 MHz carrier that the microstimulator used. A higher transmission frequency was chosen in order to improve the Q of the on-chip receiver coils. A second difference is that the mini-microstimulator requires 40 data bits (and 5 parity bits) to be transmitted per stimulation whereas the microstimulator required only 5 bits. The mini-microstimulator requires more data bits because it is a multi-channel system with much more programming flexibility. Table 7 list the 40 data bits and 5 parity bits that need to be transmitted, and Table 8 gives the order in which they need to be transmitted to the system. One parity bit comes after each 8-bit word of data, and the system uses an even parity bit scheme. In addition to the 40 data bits and 5 parity bits, two synchronization pulses needs to be sent for each stimulation output. These long duration pulses mark the beginning and end of the transmission sequence.

The required timing for the pulse width encoded data and the synchronization pulses is given in Table 9. Illustrations of the envelope for a bit=0 and bit=1 are given in Figure 14. Table 10 breaks down the timing of the entire data stream needed for stimulation, and Figure 15 illustrates the entire data stream and shows where the two timing synchronization pulses need to be. As can be seen in Figure 15, the entire data stream for each stimulation takes 5.8 mS to send. This means that the maximum stimulation frequency assuming multiple mini-microstimulators are using a single transmitter is 172 per second. If a mini-microstimulator receives a data glitch or a synchronization pulse at the wrong time in the data stream, the circuitry will revert to a reset state. Also, if the data stream does not pass parity check, the circuitry reverts to a reset state. Once all of the stimulation data is properly received by the mini-microstimulator circuitry, the system will ignore all telemetry input until it has completed both phases of the stimulation. Once stimulation is complete the circuit reverts to a reset state.
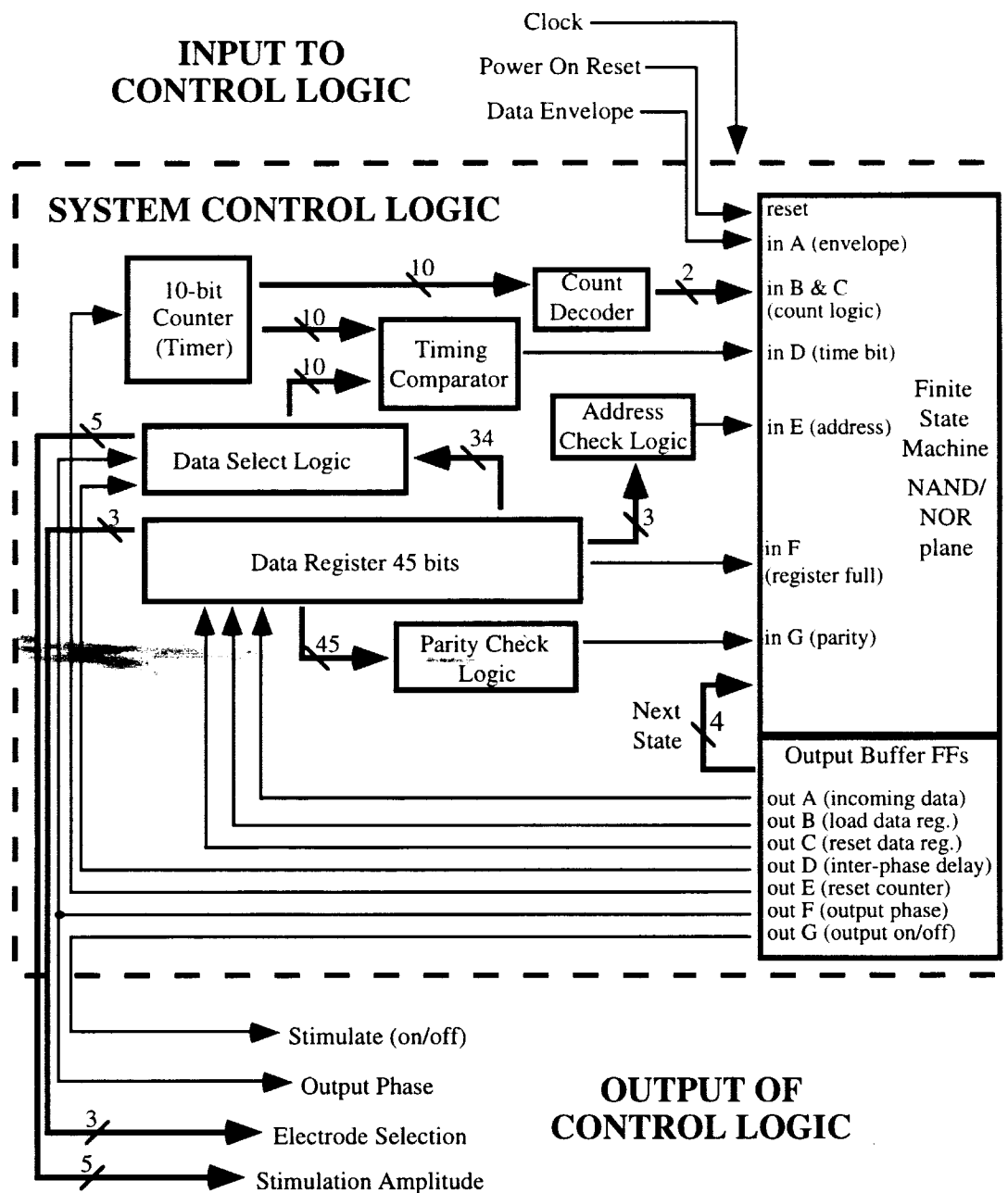
20

Clock ———
Power On Reset ———
Data Envelope ———

SYSTEM CONTROL LOGIC

10-bit Counter (Timer)		
Timing Comparator		
Count Decoder		
Data Select Logic		
Address Check Logic		
Data Register 45 bits		
Parity Check Logic		

10
10
10
5
34
3
45
2
3

reset
in A (envelope)
in B & C (count logic)
in D (time bit)
in E (address)
in F (register full)
in G (parity)

Finite
State
Machine

NAND/
NOR
plane

Next State 4

Output Buffer FFs

out A (incoming data)
out B (load data reg.)
out C (reset data reg.)
out D (inter-phase delay)
out E (reset counter)
out F (output phase)
out G (output on/off)

Stimulate (on/off)

Output Phase

Electrode Selection   3

Stimulation Amplitude   5

**OUTPUT OF
CONTROL LOGIC**

Figure 13: Block diagram of the mini-microstimulator logic

21

Table 7: The 40 data bits and 5 parity bits that need to be transmitted to the mini-microstimulator per stimulation.

Parameter	Range	Required Bits
Address of Device	Selection from up to 8 devices	3 bits
1st Phase Current Magnitude	0 to 2 mA (32 steps of 62.5 µA)	5 bits
2nd Phase Current Magnitude	0 to 2 mA (32 steps of 62.5 µA)	5 bits
Electrode Selection	Selection from 8 electrodes pairs	3 bits
1st Phase Duration	0 to 2048 µS (1024 steps of 2 µS)	10 bits
Inter-phase Delay	0 to 2048 µS (16 steps of 128 µS)	4 bits
2nd Phase Duration	0 to 2048 µS (1024 steps of 2 µS)	10 bits
Parity Bits	Even parity	5 bits
Total		*45 bits*

Table 8: The order in which the 40 data bits and 5 parity bits must be transmitted to the nerve cuff circuitry.

1	MSB of device address	16	next bit of electrode selection	31	next bit of inter-phase delay
2	next bit of device address	17	LSB of electrode selection	32	next bit of inter-phase delay
3	LSB of device address	18	parity for preceding 8 bits	33	LSB of inter-phase delay
4	MSB of phase 1 current mag.	19	MSB of phase 1 duration	34	MSB of phase 2 duration
5	next bit of phase 1 current mag.	20	next bit of phase 1 duration	35	next bit of phase 2 duration
6	next bit of phase 1 current mag.	21	next bit of phase 1 duration	36	parity for preceding 8 bits
7	next bit of phase 1 current mag.	22	next bit of phase 1 duration	37	next bit of phase 2 duration
8	LSB of phase 1 current mag.	23	next bit of phase 1 duration	38	next bit of phase 2 duration
9	parity for preceding 8 bits	24	next bit of phase 1 duration	39	next bit of phase 2 duration
10	MSB of phase 2 current mag.	25	next bit of phase 1 duration	40	next bit of phase 2 duration
11	next bit of phase 2 current mag.	26	next bit of phase 1 duration	41	next bit of phase 2 duration
12	next bit of phase 2 current mag.	27	parity for preceding 8 bits	42	next bit of phase 2 duration
13	next bit of phase 2 current mag.	28	next bit of phase 1 duration	43	next bit of phase 2 duration
14	LSB of phase 2 current mag.	29	LSB of phase 1 duration	44	LSB of phase 2 duration
15	MSB of electrode selection	30	MSB of inter-phase delay	45	parity for preceding 8 bits

Table 9: The time constraints on the data envelope for signals sent to the mini-microstimulator.

State of Envelope	Time	Meaning of Counter State
High	0-3 µS	Glitch (not valid data)
	4-63 µS	Time high for transmitted Bit=0
	64-127 µS	Time high for transmitted Bit=1
	>127 µS	Sync1 signal
Low	0-3 µS	Glitch (not valid data)
	4-63 µS	Time low for transmitted Bit=1
	64-127 µS	Time low for transmitted Bit=0
	>127 µS	Sync2 signal

Table 10: The nominal time required to transmit the full data stream needed for stimulation.

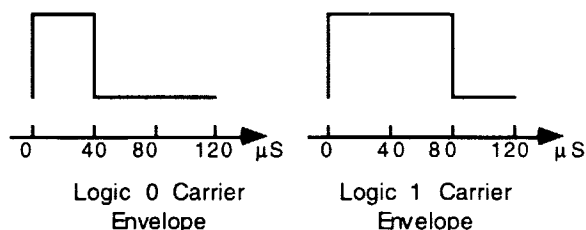| Transmitted Signal	Transmission Time
Sync1 Pulse	0.2 mS
40 data + 5 parity bits (each bit)	5.4 mS (120 µS)
Sync2 Pulse	0.2 mS
Total	*5.8 mS* *(172 per sec)*

Logic 0 Carrier Envelope   Logic 1 Carrier Envelope

Figure 14: The nominal carrier for a transmitted bit=1 and bit=0.
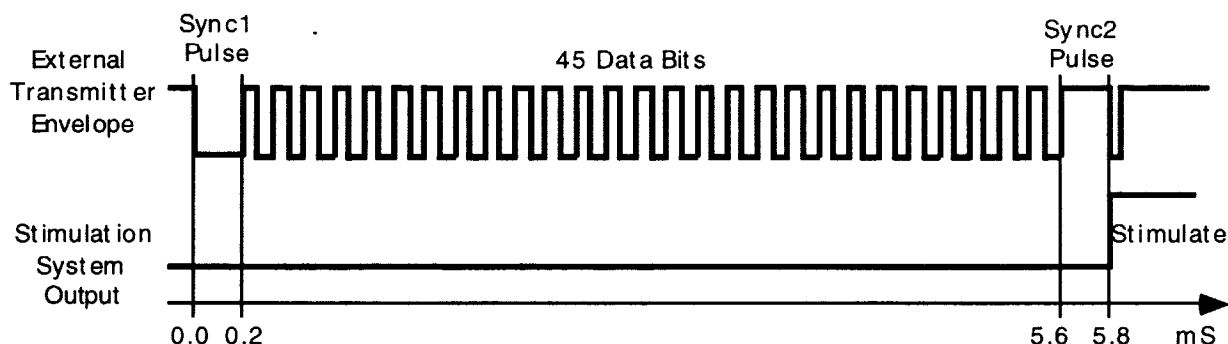
Figure 15: The nominal timing for complete data stream sent for each stimulation pulse.

2.3.3 On-Chip Receiver Coils

This quarter we fabricated one new type of on-chip coil to help improve our understanding and modeling of these devices. This new design is not a fully integrated on-chip coil, but rather an on-chip coil with a discrete commercial ferrite core (μ_{rel}=125 at 4 MHz). This design was fabricated to enable us to compare the performance of our electroplated NiFe cores to a high quality commercial core. Figure 16 reviews the on-chip coil designs that have been fabricated so far, along with the new one that was fabricated and measured this quarter. Table 11 shows inductance, impedance, and Q measurements from each of these designs. Recall that design D is the best performing fully integrated design. A 10-turn version of this design has an inductance of 2.7 µH, a resistance of less than 10 Ω, and a Q of well over 6. As can be seen, an identical coil with a

23

commercial ferrite core as shown in design E has an inductance of 2.91 μH, and a Q of 7.3. The commercial core only gave about a 10% increase in inductance and Q over an electroplated NiFe core, even through the commercial core was 500 μm thick while the electroplated NiFe cores are 10 μm thick. Although the discrete commercial ferrite core performed slightly better than the fully integrated design D, it complicates assembly and doubles the thickness of the coil, resulting in a much larger volume implant. For these reasons we feel that the fully integrated design D is the better choice for the mini-microstimulator.
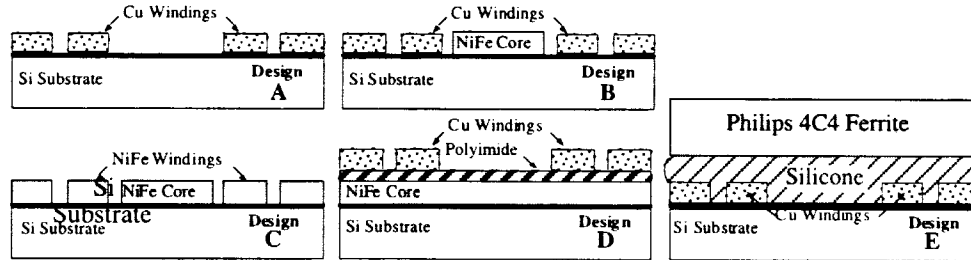

Figure 16: The five different planar on-chip coil designs that have been fabricated. Design D is the best performing fully integrated design, and design E is a slightly better performing design fabricated this quarter.

Table 11: Measurements from 10 turn versions of each of the coil designs shown in Fig. 16.

Design	A	B	C	D	E
Inductance	2.70μH	0.95μH	0.99μH	9.0μH	2.91μH
Resistance	10Ω	9.6Ω	9.6Ω	160Ω	10Ω
Q(f$_t$=4MHz)	6.6	2.5	2.6	1.4	7.3

Figure 17 shows a cross-sectional SEM of one of the fabricated on-chip coils of design D. As can be seen, the NiFe core is very close to its target thickness of 10 μm, and the polyimide insulation layer is about 7 μm. This quarter we measured the self resonance of these coils and found that the 2.7 μH, 10 turn design had a self resonance of over 40 MHz. This high self resonance is largely due to the thick polyimide dielectric layer under the windings, which minimizes capacitance to the underlying layers.

3. ACTIVITIES PLANNED FOR THE COMING QUARTER

Our efforts on the various aspects of this project will continue in the coming quarter. First, we will continue our soak tests of glass-silicon packages and we will start some new tests in this quarter. These tests will be performed on both the large and the flat glass package. We are still developing techniques by which we can overcome or circumvent the problem of silicon dissolution in saline solutions at high temperatures. Once this is done we will be able to conduct additional tests at high temperatures. In-vivo tests using the silicon-glass packages will also continue and we will report on the results of these tests as they become available.

24

In the area of microstimulator development and testing, our main objective remains to be the determination of the source of high leakage current in our latest batch of devices. A large number of tests have already been performed, and another series of tests will be carried out to determine the source of this problem. We will fabricate another set of devices using a new mask set that incorporates changes to reduce the leakage current.

Finally, in the coming quarter we will lay out and fabricate the complete nerve cuff mini-microstimulator circuitry that was designed during the past few months. We will include the latest version of the single channel microstimulator circuitry and the multi-channel microstimulator circuitry in this run. We plan to complete the fabrication of this circuitry this summer.
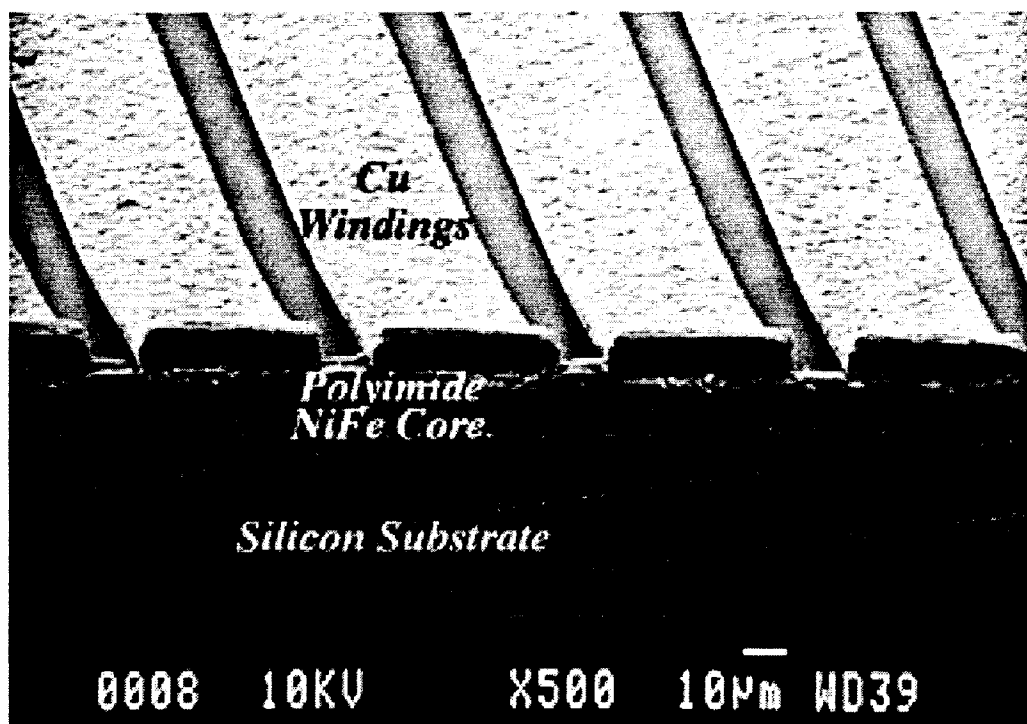

Figure 17: A SEM showing a cross-section of one of the coils of design D in Fig. 30.